Available online at www.sciencedirect.com
SCIENCE DIRECT®
Biochemical Pharmacology 67 (2004) 631–642
Biochemical Pharmacology
www.elsevier.com/locate/biochempharm

Antitumor AZA-anthrapyrazoles: biophysical and biochemical studies on 8- and 9-aza regioisomers

Claudia Sissi[a,*], Elisabetta Leo[a], Stefano Moro[a], Giovanni Capranico[b], Annalaura Mancia[b], Ernesto Menta[c], A. Paul Krapcho[d], Manlio Palumbo[a]

[a]*Department of Pharmaceutical Sciences, University of Padova, Via Marzolo, 5, 35131 Padova, Italy*
[b]*Department of Biochemistry, University of Bologna, Via Irnerio 48, 40126 Bologna, Italy*
[c]*Novuspharma, SpA, Bresso (MI), Italy*
[d]*Chemistry Department, University of Vermont, 05405 Burlington, VT, USA*

Received 9 July 2003; accepted 17 September 2003

Abstract

Aza-bioisosteres of anthrapyrazoles (Aza-APs) bearing the C–N substitution at position 9 are powerful anticancer agents now in clinical trials. In contrast, their 8-substituted regioisomers are practically devoid of chemotherapeutic effects. To understand the molecular basis for a dramatically different response by otherwise very similar compounds, we performed a detailed investigation on the physico-chemical properties of several aza-APs belonging to the two families, on their DNA-binding affinity and specificity as well as on their capacity to impair the activity of the two isoforms of human Topoisomerase II (top2α and top2β). Our results indicate that molecular size and shape, electronic distribution, redox properties, lipophilicity and protonation equilibria are essentially the same when comparing 9- with 8-substituted congeners. Although no major difference could be picked up when comparing the DNA binding properties of corresponding members of the 8- and 9-aza families, interestingly the affinity and specificity for the nucleic acid is modulated by the nature of the side-arms linked to the aza-AP scaffold, suggesting structural motifs that may determine DNA sequence recognition by the studied drug. Topoisomerase II poisoning activity was much higher for 9-aza derivatives than 8-aza analogues as shown by a cleavage assay with purified recombinant top2 isoforms. The difference appears to account for the divergent anticancer potential exhibited by different aza-AP regioisomers and suggests a specific molecular recognition of the cleavage complex by the studied drugs.

Keywords: AZA-APs; Regioisomers; Topoisomerase II; DNA binder

1. Introduction

Aza-anthracenediones represent a successful example of the application of bioisosterism in the optimization of a lead structure [1]. This family of compounds is structurally related to mitoxantrone (MX), a clinically useful anticancer drug, whose mechanism of action is mainly related to the poisoning of the DNA Topoisomerase II enzyme [2,3]. By freezing the enzyme-DNA cleavage complex through effective interactions, MX induces an extensive DNA fragmentation and, as a consequence, activation of apoptotic pathways. One of the major problems with the clinical use of MX and congeners is related to cardiotoxic effects induced by a prolonged treatment. Indeed, MX can undergo redox cycling, giving rise to accumulation of free radical species at the cardiac level [4]. To overcome this important drawback, a nitrogen atom has been introduced into the carbocyclic aromatic planar system in an attempt to reduce redox potential and free radical production by the drug [5–7]. Extensive synthetic work associated to thorough pharmacological studies have led to the discovery of the novel potent 2-aza anthracenedione, pixantrone (formerly BBR 2778), that associates anticancer activity with significantly reduced cardiotoxicity, as shown by early clinical trials [8–10].

An alternative approach to reduce redox cycling has led to the development of anthrapyrazoles, in which a pyrazole ring is fused to the anthraquinone moiety, giving a

* Corresponding author. Tel.: +39-049-8275711; fax: +39-049-8275711.
E-mail address: claudia.sissi@unipd.it (C. Sissi).

0006-2952/$ – see front matter © 2003 Elsevier Inc. All rights reserved.
doi:10.1016/j.bcp.2003.09.035

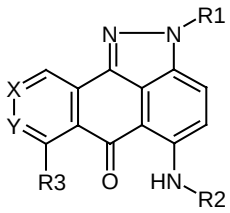

COMPOUND	X	Y	R1	R2	R3	LoVo[a]	LoVo/DX[a]
LX	-CH=	-CH=	-$(CH_2)_2NH(CH_2)_2OH$	-$(CH_2)_2NH(CH_2)_2OH$	-OH	0.053	44.5
BBR 3438	-N=	-CH=	-$(CH_2)_2NH(CH_2)_2OH$	-$(CH_2)_2NH(CH_3)$	-H	0.54	>100
BBR 3576	-N=	-CH=	-$(CH_2)_2NH(CH_2)_2OH$	-$(CH_2)_2N(CH_3)_2$	-H	0.3	57
BBR 3387	-N=	-CH=	-$(CH_2)_2NH_2$	-$(CH_2)_2NH_2$	-H	0.86	15.4
BBR 3530	-N=	-CH=	-$(CH_2)_2NH(CH_3)$	-$(CH_2)_2NH(CH_3)$	-H	0.04	2.5
BBR 3378	-N=	-CH=	-$(CH_2)_2N(CH_3)_2$	-$(CH_2)_2N(CH_3)_2$	-H	0.35	1.0
BBR 3421	-N=	-CH=	-$(CH_2)_2NH(CH_2)_2OH$	-$(CH_2)_2NH(CH_2)_2OH$	-H	4.5	>100
BBR 3556	-N=	-CH=	-$(CH_2)_2NH(CH_2)_2OH$	-$(CH_2)_2N(CH_3)_2$	-OH	0.010	0.93
BBR 3599	-N(-O)=	-CH=	-$(CH_2)_2NH(CH_2)_2OH$	-$(CH_2)_2N(CH_3)_2$	-H	3.2	>100
BBR 3388	-CH=	-N=	-$(CH_2)_2NH_2$	-$(CH_2)_2NH_2$	-H	12.8	>100
BBR 3412	-CH=	-N=	-$(CH_2)_2NH(CH_2)_2OH$	-$(CH_2)_2NH(CH_2)_2OH$	-H	>100	>100
BBR 3588	-CH=	-N=	-$(CH_2)_2NH(CH_2)_2OH$	-$(CH_2)_2NH(CH_3)$	-H	24.9	>100
BBR3587	-CH=	-N=	-$(CH_2)_2NH(CH_2)_2OH$	-$(CH_2)_2N(CH_3)_2$	-H	33.9	>100

[a] Compound used in the dihydrochloride form

[b] Compound used in the dimaleate form

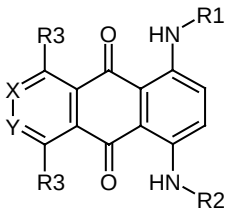

COMPOUND	X	Y	R1	R2	R3	LoVo[a]	LoVo/DX[a]
MX	-CH=	-CH=	-$(CH_2)_2NH(CH_2)_2OH$	-$(CH_2)_2NH(CH_2)_2OH$	-OH	0.023	0.62

[a] : data from reference [14]

Scheme 1. Chemical structure and cytotoxicity of test compounds.

tetracyclic system. In this class one derivative, losoxantrone (LX), has emerged as a promising clinical candidate [11]. Although this compound demonstrated good clinical efficacy in the treatment of breast cancer, high levels of cardiac toxicity were still observed during clinical trials [12,13].

Combining the approaches of bioisosteric substitution with pyrazole introduction into the anthraquinone system led to the design of aza-anthrapyrazoles. C–N substitutions were introduced at different positions of the anthrapyrazole ring system, giving different regioisomers [14]. Interestingly, and in analogy to aza-anthracenediones, the cytotoxic properties of these derivatives were substantially affected by the location of the bioisosteric nitrogen. In fact, only 9-aza derivatives showed outstanding activity both *in vitro* and *in vivo*, whereas all other bioisosteres, in particular those substituted at position 8, were essentially inactive (see Scheme 1). In a previous investigation, we closely examined two pharmacologically relevant 9-aza anthrapyrazoles now in Phase II clinical studies (BBR 3438 and BBR 3576) and showed that bioisosteric substitution plays an important role in defining the physicochemical properties and in modulating the affinity of anthrapyrazoles for DNA, the geometry of the intercalation complex and the sequence specific contacts along the DNA chain [15]. In addition, it emerged that drug stimulation of Topoisomerase II-mediated DNA cleavage was attenuated in the aza derivatives when compared to their carbocyclic analogues.

To further understand the mechanism of action of aza anthrapyrazole (aza-AP) and the absolute requirement for a nitrogen atom at position 9, in this paper we will extend our structure–activity relationship investigation to a number of novel 9-aza derivatives and compare them with several

8-substituted congeners. Their chemical structures are reported in Scheme 1. In particular, we will examine and compare the physico-chemical properties of the test aza-APs together with their DNA-binding affinity, geometry and sequence selectivity. In addition, we will investigate the interference of aza-APs with the catalytic cycle of recombinant human Topoisomerase II α and β isoforms.

2. Materials and methods

2.1. Materials

Aza-APs were synthesized as previously described [16]. Losoxantrone (LX) was synthesized according to the published procedure [17]. Mitoxantrone (MX) was a generous gift of Lederle. Stock solutions (1 mg mL^{-1}) of test compounds were prepared in deionized water and diluted to the appropriate concentration in the working buffer prior to use.

DNA from calf thymus (ctDNA, highly polymerized sodium salt) was purchased from Sigma. Synthetic alternating polynucleotides poly(dG-dC) and poly(dA-dT) were purchased from Eurogentec and annealed prior to use. Their concentrations were determined applying the molar extinction coefficients per residue of 6600, 6800, and 8400 M^{-1} cm^{-1}, respectively [18,19].

Human recombinant Topoisomerase II α and β were purified from overexpressing yeast strains as previously reported [20,21].

α[^{32}P]ATP (6000 Ci $mmol^{-1}$) was obtained from NEN. All DNA modifier enzymes were purchased from Gibco and used according to the supplier's recommended protocol in the activity buffer provided.

All other chemicals were analytical grade reagents, and all solutions were prepared using doubly deionized, Millipore filtered water.

2.2. DNA binding studies

Fluorometric measurements were performed with a Perkin-Elmer LS30 fluorometer, equipped with a Haake F3-C thermostat. Spectrophotometric titrations were performed with a Perkin-Elmer Lambda 20 apparatus. Titrations were carried out at 25° in ETN (1 mM EDTA, 10 mM Tris–HCl, pH 7.0, and NaCl to obtain the desired ionic strength). Binding was followed by addition of increasing amounts of DNA to a freshly prepared drug solution. To avoid large systematic inaccuracies due to experimental errors, the range of bound drug fractions utilized for calculations was 0.15–0.85. Data were evaluated according to the equation of McGhee and Von Hippel [22] for noncooperative ligand–lattice interactions:

$$\frac{r}{m} = \frac{K_i(1-nr)^n}{[1-(n-1)r]^{n-1}}$$

where r is the molar ratio of bound ligand to DNA, m is the free ligand concentration, K_i the intrinsic binding constant, and n the exclusion parameter.

2.3. DNA unwinding

DNA unwinding induced by drug binding was monitored following the changes in electrophoretic mobility of supercoiled pBR322 in the presence of different drug/DNA ratio. In a total volume of 20 μL, of 10 mM Tris, 1 Mm EDTA, 50 mM KCl, pH 7.0, 0.15 μg of plasmid were incubated with increasing concentrations of test drug. After 15 min at room temperature, samples were loaded onto a 1% agarose gel in TBE (89 mM Tris-base, 89 mM boric acid, 2 mM Na_2EDTA) and run at 5 V/cm for 3.5 hr. DNA was stained with ethidium bromide and gels photographed under UV light.

2.4. Chiroptical studies

Circular dichroism spectra were recorded on a Jasco 710 spectropolarimeter. Quartz cells having 10 mm pathlength were used. Up to four scans were accumulated for each measurement.

2.5. Computational methodologies

Calculations were performed on a Silicon Graphics Octane R12000 workstation and on an Intel PIV 2.4 GHz machine. This study involved the use of consensus dinucleotide intercalation geometries d(ApT) and d(GpC) initially obtained using NAMOT2 (Nucleic Acid Modeling Tool) software. d(ApT) and d(GpC) intercalation sites were contained in the center of a decanucleotide duplex of sequences d(5′-ATATA-3′)$_2$ and d(5′-GCGCG-3′)$_2$, respectively. Decamers in B-form were built using the ''DNA Builder'' module of Molecular Operating Environment (MOE 2001.01). Decanucleotides were minimized using Amber94 all-atom force field, implemented by MOE modeling package, until the *rms* value of Truncated Newton method (TN) was <0.001 kcal mol^{-1} $Å^{-1}$. The dielectric constant was assumed to be distance independent with a magnitude of 4.

The ground state geometry of aza-anthrapyrazole structures were fully optimized without geometry constraints using RHF/3-21G(*) *ab initio* calculations. Vibrational frequency analysis was used to characterize the minima stationary points (zero imaginary frequencies). RHF/AM1-SM5.4 method has been used for treatment of molecules in water [23]. The software package Spartan O2 was utilized for all quantum mechanical calculations. Molecular descriptors such as log P and ΔH_{hyd} have been calculated using MOE suite. Aza-anthrapyrazole derivatives were docked into both intercalation sites using flexible MOE-Dock methodology. The purpose of MOE-Dock is to search for favorable binding configurations between a

small, flexible ligand and a rigid macromolecular target. Searching is conducted within a user-specified 3D docking box, using simulated annealing protocol and Amber94 force field. MOE-Dock performs a user-specified number of independent docking runs (55 in our specific case) and writes the resulting conformations and their energies to a molecular database file. The resulting DNA-drug intercalated complexes were subjected to Amber94 all-atom energy minimization until the *rms* of conjugate gradient was <0.1 kcal mol^{-1} $Å^{-1}$. Charges for the ligands were imported from the Spartan output files. To model the effects of solvent more directly, a set of electrostatic interaction corrections are used. MOE suite implemented a modified version of GB/SA contact function described by Still and coworkers [24]. These terms model the electrostatic contribution to the free energy of solvation in a continuum solvent model. The interaction energy values were calculated as the energy of the complex minus the energy of the ligand, minus the energy of DNA: $\Delta E_{\text{inter}} = E_{(\text{complex})} - (E_{(L)} + E_{(\text{rDNA})})$.

2.6. Topoisomerase II assay

Plasmid pBR322 was first restricted with *Eco*RI, and then 3′-end-labeled with Klenow fragment and α[^{32}P]ATP. After phenol–chloroform extraction and ethanol precipitation, DNA was digested with *Hin*dIII, and uniquely 3′-end-labeled DNA fragments were then purified on a microspin G-25 column and used without further purification. DNA (50 ng) was incubated with 1.2 U of Topoisomerase II in a total volume of 20 μL with or without drugs in 50 mM Tris–HCl, pH 8.0, 120 mM KCl, 10 mM $MgCl_2$, 0.5 mM ATP, 0.5 mM DTT, and 30 μg mL^{-1} BSA for 30 min at 37°. Reactions were stopped by adding of 1% SDS, 0.5 mg mL^{-1} protein kinase, 1 ng cold DNA and followed by an incubation for 60 min at 50°. DNA cleavage was analyzed with 1% agarose gel in TBE. Dried gels were then exposed to Amersham Hyperfilm MP at −70° with intensifying screens.

3. Results

3.1. Physico-chemical properties of aza-APs

3.1.1. Spectroscopic characterization

All aza-APs exhibit visible absorption bands in the 450–550 nm range in ETN buffer, pH 7.0. Corresponding 8- and 9-aza-substituted isomers showed closely comparable locations and intensities (not shown). No significant deviations from linearity of plots Absorption vs. concentration were observed up to 10^{-4} M drug. Additionally, when irradiated at the maximum absorption wavelength, aza-APs produced intense fluorescence responses. This allowed us to investigate the behavior of the test drugs at physiologically significant concentrations (μM range). The only exception is represented by the hydroxylated derivative BBR 3556. This compound is not fluorescent and a modest variation of its extinction coefficient was observed upon increasing drug concentration. In analogy to previously reported data on anthrapyrazole congeners, the presence of an hydroxyl group seems to favor self-aggregation processes [25].

3.2. Protonation equilibria

The test aza-APs are characterized by four potential protonation sites: the two differently substituted amino groups in the side chains, the bioisosteric nitrogen and one nitrogen on the pyrazole ring. To assess the effects of the bioisosteric nitrogen position on the protonation equilibria of aza-APs, spectrophotometric studies were performed as a function of pH. Representative results are reported in Fig. 1, where the 8-aza derivative BBR 3388 is compared to the 9-aza analogue BBR 3387. The absorption spectra of both derivatives are extremely sensitive to pH, reflecting a correlation between the optical properties of aza-APs and their protonation state. Interestingly, the plots in Fig. 1 are almost superimposable. Hence, the position of the C–N substitution does not affect protonation equilibria to a significant extent. The same holds true for the other compounds under investigation (data not shown).

3.3. Theoretical calculations

A molecular modeling study has been carried out to better depict the crucial differences concerning the chemical and pharmacological behavior of 8- and 9-aza-anthrapyrazole derivatives. Obviously, from the structural point of view both isomers present identical steric requirements and hydrophobic behaviors, as clearly shown analyzing the corresponding values of molecular surface, volume, log *P*, and ΔH_{hyd} energies (see Table 1). Also considering the corresponding electronic properties (e.g. HOMO and LUMO energies) the two isomers seem to be very similar. As clearly explained later, symmetries and energies of molecular orbitals, especially HOMO and LUMO, are crucial to determine the chemical properties of chemical structures, and in particular the redox behavior of these aza-anthrapyrazole derivatives. Another interesting

Table 1
Calculated physico-chemical properties of aza-anthrapyrazoles

	Compound	
	BBR 3387	BBR 3388
Total dipole (debye)	6.06	6.89
HOMO (eV)	−8.34	−8.38
LUMO (eV)	−1.23	−1.25
Surface area ($Å^2$)	365.9	365.9
Molecular volume ($Å^3$)	358.9	358.9
ΔH_{hyd} (kcal mol^{-1})	−20.9	−21.7
log *P* (Ghose–Crippen)	−0.52	−0.52

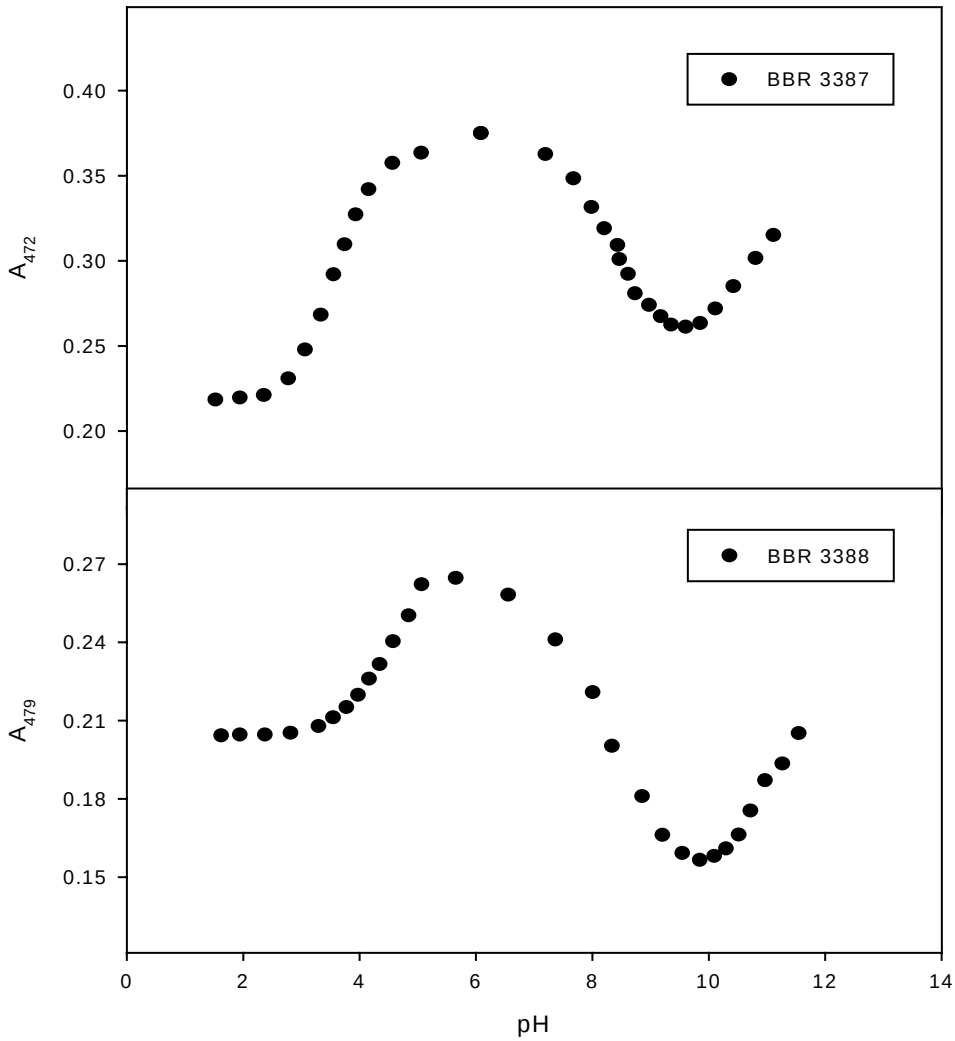

Fig. 1. Plot of absorbance changes at 472 or 479 nm for BBR 3387 and BBR 3388, respectively, as a function of pH in 50 mM NaCl, 25°.

comparison concerns the protonation of the aza-anthrapyrazole system. AM1-SM5.4 semiempirical calculations have been used to investigate the basicities the aza-anthrapyrazole nitrogen atoms of both 8- and 9-aza-anthrapyrazole isomers in water. As shown in Fig. 2, no major differences have been observed between the two isomers in their acid–base properties.

3.4. Aza-APs binding to DNA

3.4.1. Binding affinity

Upon addition of DNA, the optical properties of all test compounds undergo substantial modifications (Fig. 3). Generally, changes in fluorometric responses were used to quantitatively evaluate the DNA binding process. For the

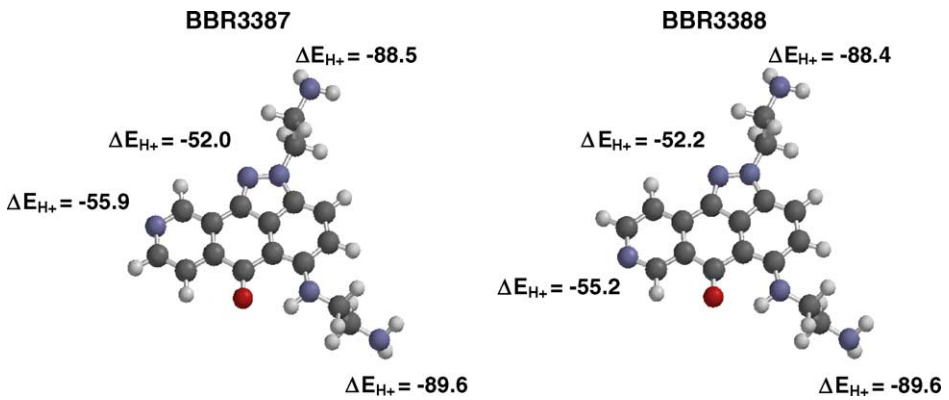

Fig. 2. Calculated energies for the protonation of basic nitrogen sites in BBR 3388 and BBR 3387.

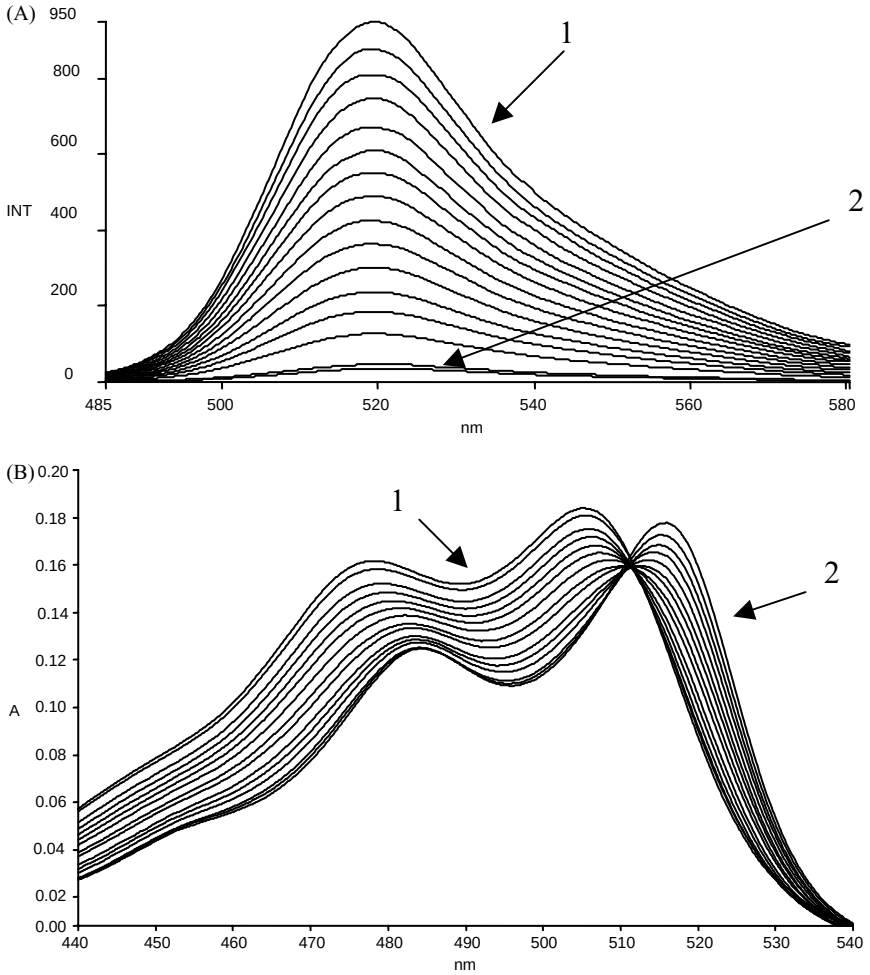

Fig. 3. Optical properties changes of BBR 3421 (fluorometric titration, panel A) and of BBR 3556 (spectrophotometric titration, panel B) upon addition of increasing amounts of DNA in ETN 0.1 M, pH 7.0, 25°. Curve 1: free drug; curve 2: fully bound drug.

nonfluorescent derivative BBR 3556, spectrophotometric titrations were performed. Analysis of the binding data according to the McGhee and Von Hippel formalism yielded the thermodynamic parameters summarized in Table 2. For all derivatives the exclusion parameter was always close to two base pairs, consistent with an intercalation binding mode.

Table 2
DNA binding constants (K_i, M^{-1}) of test compounds to nucleic acids having different base composition in ETN buffer, 0.1 M ionic strength, pH 7.0, 25°

Compound	ctDNA	Poly(dG-dC)	Poly(dA-dT)
LX	5.64 ± 0.37	3.73 ± 0.13	0.55 ± 0.01
BBR 3438	12.3 ± 0.94	23.2 ± 1.42	≈0
BBR 3576	11.45 ± 1.35	29.00 ± 1.15	≈0
BBR 3387	6.60 ± 0.18	9.41 ± 0.32	2.99 ± 0.23
BBR 3530	6.05 ± 0.25	6.57 ± 0.18	≈0
BBR 3378	6.13 ± 0.12	7.23 ± 0.12	≈0
BBR 3421	9.93 ± 0.45	11.23 ± 0.57	≈0
BBR 3556	3.07 ± 0.44	2.30 ± 0.15	0.34 ± 0.02
BBR 3599	2.77 ± 0.16	3.40 ± 0.15	≈0
BBR 3388	9.30 ± 0.29	13.11 ± 0.40	3.03 ± 0.20
BBR 3412	10.44 ± 0.59	11.96 ± 0.65	≈0
BBR 3588	8.88 ± 0.61	11.74 ± 0.70	2.32 ± 0.15
BBR 3587	8.34 ± 0.59	11.07 ± 0.64	≈0

The exclusion parameter, n, was always close to two base pairs.

The methylation degree of the terminal amino group did not affect DNA affinity to a significant extent. A 2-fold increment in K_i was observed when at least one side chain is an hydroxy-ethylamino-ethyl group. When this group was present at position 5 of the planar ring system, the nature of the second side chain did not remarkably affect DNA binding properties of the aza-APs.

A drop in K_i value was observed both when an hydroxyl group was introduced into the chromophore (BBR 3556) or when the isosteric nitrogen was present as the N-oxide (BBR 3599). Indeed, the latter two derivatives showed binding constants even lower than LX. This is a peculiar behavior as in the anthraquinone family the DNA affinity is substantially increased upon insertion of hydroxyl group(s) in the planar ring system [26,27].

3.4.2. Sequence specificity of DNA binding

Both the nature of the side chains and the position of the nitrogen atom in the planar ring system can influence recognition of specific DNA sites by aza-APs. Selective

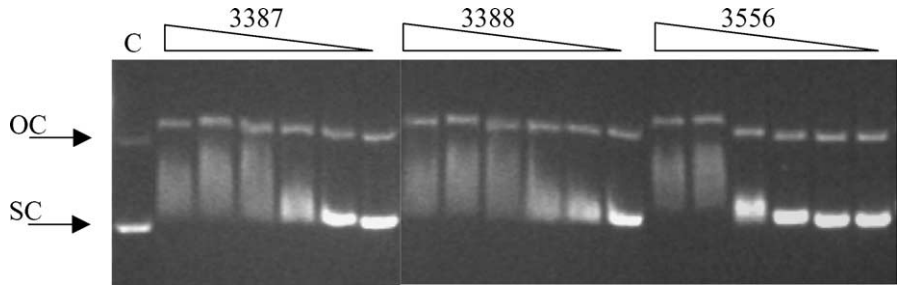

Fig. 4. Unwinding of pBR322 in the presence of increasing amounts of BBR 3556, BBR 3388, or BBR 3387. DNA was incubated with 0.1, 0.5, 1.0, 5.0, 10, 50 μM of each drug for 15 min at room temperature in 10 mM Tris, 1 mM EDTA, 50 mM KCl before loading onto agarose gel. Lane C refers to DNA in the absence of drug, OC and SC to open circular and supercoiled pBR322 form, respectively.

binding along the genome would possibly affect both drug potency and toxicity. Thus, the binding properties of the test drugs to DNAs having different base pair composition were evaluated. Results are summarized in Table 2.

All test aza-APs showed remarkable preference for alternating dG-dC sequences, binding more efficiently to these than to dA-dT sequences or to natural ctDNA. The only exception is represented by the hydroxylated derivative BBR 3556, which did not prefer alternating GC or AT sequences. Interestingly, the pharmacologically most relevant BBR 3438 and BBR 3576 were the best binders for poly(dG-dC). All other test derivatives showed a 1.2–1.4-fold increase in K_i with this sequence as compared to ctDNA. Additionally, an interesting modulation in the binding emerged using poly(dA-dT). In fact, some of the compounds showed vanishing low affinity for this sequence. In particular, binding was not even detectable using compounds (both 8- and 9-aza derivatives) with bulky side-arms (tertiary amines as in BBR 3438 and BBR 3599).

3.5. Mode of interaction with DNA

3.5.1. Electrophoretic mobility

The mode of interaction of the test derivatives with DNA has been evaluated examining their ability to affect the electrophoretic mobility of supercoiled plasmid DNA. In the presence of aza-APs, a bell-shaped dependence of plasmid mobility in the gel occurred upon increasing drug concentration (Fig. 4). Hence, we can safely conclude that 8- and 9-aza-APs intercalate into the DNA double helix similarly to the parent carbocyclic drug LX.

3.5.2. Orientation of the intercalated chromophore: chiroptical studies

The orientation of the aza-anthrapyrazole chromophore in the intercalation complex was investigated examining circular dichroism signal induced in the visible region upon drug binding to DNA. In particular, we studied the role of the position of the C–N bioisosteric substitution in the complex geometry comparing the dichroic signal induced when the bioisosteres bind to the alternating synthetic

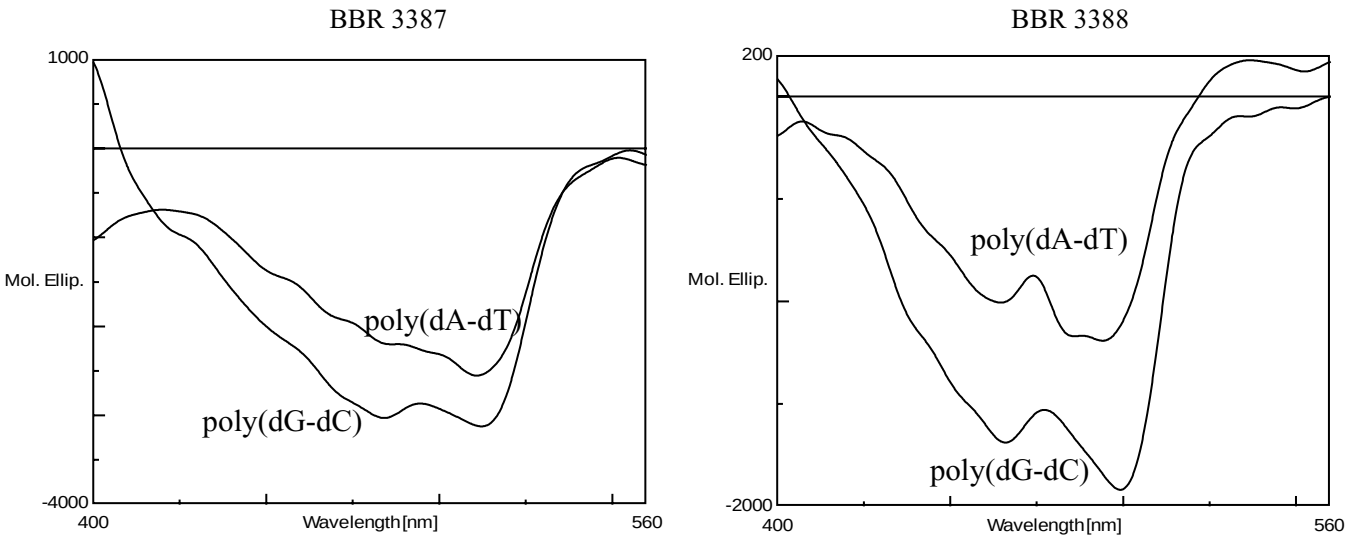

Fig. 5. Circular dichroism induced in the visible region by the binding of BBR 3388 and BBR 3387 to poly(dG-dC) or poly(dA-dT) in ETN 0.1 M, pH 7.0, 25°. DNA base to drug ratios were of the order of 25, drug concentrations were 10^{-5} M.

polynucleotides poly(dG-dC) and, when possible, poly(dA-dT). A negative induced rotational strength was always monitored. The results obtained using compounds BBR 3387 and BBR 3388 are reported as an example in Fig. 5.

It is worth noting that, according to theoretically derived dichroic maps, a negative rotational strength with AT or GC containing polynucleotides possibly corresponds to different intercalation geometries [28,29]. In fact, in the presence of poly(dA-dT), our data are compatible with a chromophore orientation parallel to the DNA base pair hydrogen bonding direction. In this case, one side chain of the drug would lay in the major groove and the other in the minor groove. This is consistent with the extremely reduced AT binding affinity observed with derivatives carrying bulky side chains (tertiary amines) that can hardly slide across two adjacent base pairs to reach a straddling intercalation mode. On the other side, a negative induced dichroic signal in the case of poly(dG-dC) is compatible with an intercalation of the drug chromophore perpendicular to the base pair longest dimension, with both side chains lying in the same groove.

3.5.3. Orientation of the intercalated chromophore: molecular modeling studies

Further insight into the structure of the DNA intercalation complexes generated by aza-APs was obtained by means of molecular modeling studies. The most energetically favorable conformations assumed by BBR 3387 and BBR 3388 when intercalated into poly(dA-dT) and poly(dG-dC) were explored using a flexible docking protocol. The docking data with complexes of both DNA sequences show that aza-APs may adopt two different orientations of the intercalated chromophore as function of the nature of the duplex. In the presence of poly(dA-dT), the most stable and representative docked conformation of both 8- and 9-aza-anthrapyrazole derivatives shows a chromophore orientation parallel to the DNA base pair axes, with one side chain in each groove (Fig. 6A). *Vice versa*, in the presence of poly(dG-dC), a perpendicular

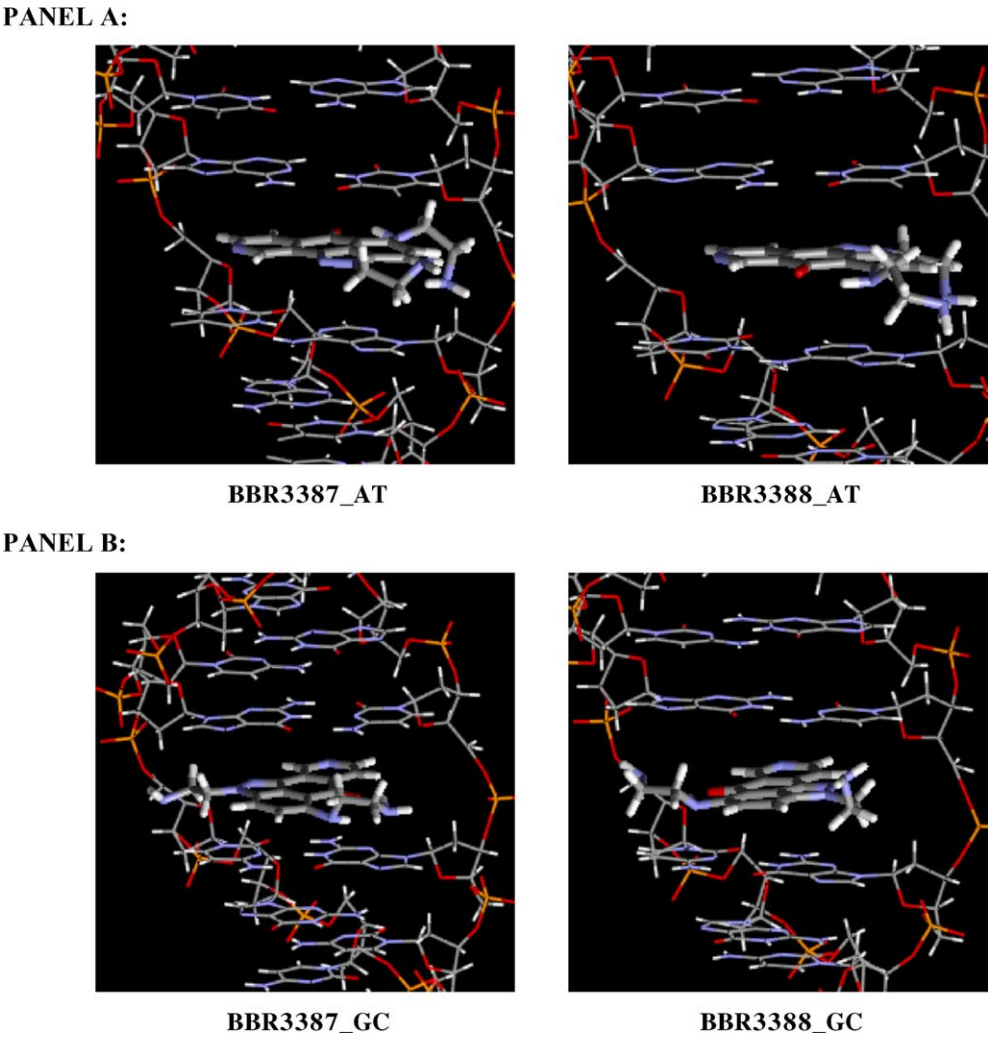

Fig. 6. Preferred structures of aza-anthrapyrazole derivatives BBR 3388 and BBR 3387 intercalated between dA-dT (A) or dG-dC (B) steps as determined by molecular modeling.

intercalation of the aza-AP moiety is preferred, with both side chains located in the major groove (see Fig. 6B). Moreover, taking into account both aza-AP derivatives, the intercalation into GC steps (−106.2 and −104.6 2 kcal mol^{-1} for BBR 3387 and BBR 3388, respectively) is energetically more favorable than the one between AT steps (−87.2 and −95.7 kcal mol^{-1} for BBR 3387 and BBR 3388, respectively). Considering the energy components of the Amber force field used in the scoring step of the docking protocol, the maximization of the electrostatic energy term seems to account for the change of aza-APs orientation when intercalated into AT or GC steps. Adopting parallel or perpendicular orientation, respectively, both aza-AP derivatives can optimize the coulomb interactions among the planar aza-anthrapyrazole moiety and the adjacent DNA base pairs, and also the electrostatic interactions between the positively charged side chains of both aza-APs and the negatively charged phosphate groups of the DNA duplex. These results are fully consistent with the chiroptical data experimentally obtained.

3.6. Human DNA-Topoisomerase II poisoning

3.6.1. Stimulation of Topoisomerase II-mediated DNA cleavage

The poisoning properties of the test drugs on the human DNA Topoisomerase II (top2) α and β isoforms were investigated by monitoring the enzyme-mediated stimulation of DNA cleavage.

In agreement with previous reported data on BBR 3438, BBR 3576 and related compounds [15,25], all test compounds, when incubated with DNA do not induce breakage *per se* (data not shown). However, in the presence of top2α they stimulate DNA cleavage in a concentration dependent fashion, with maximal activity close to 1 μM (Fig. 7A).At the highest concentrations used, a general suppression of the cutting activity was observed, according to known effects of strong DNA binders [15]. Compared to MX, LX and 9-aza derivatives induced weaker stimulation of DNA cleavage mediated by top2α isoform. The most effective derivative was BBR 3556 that stabilizes the cleavage complex to an extent comparable to LX.

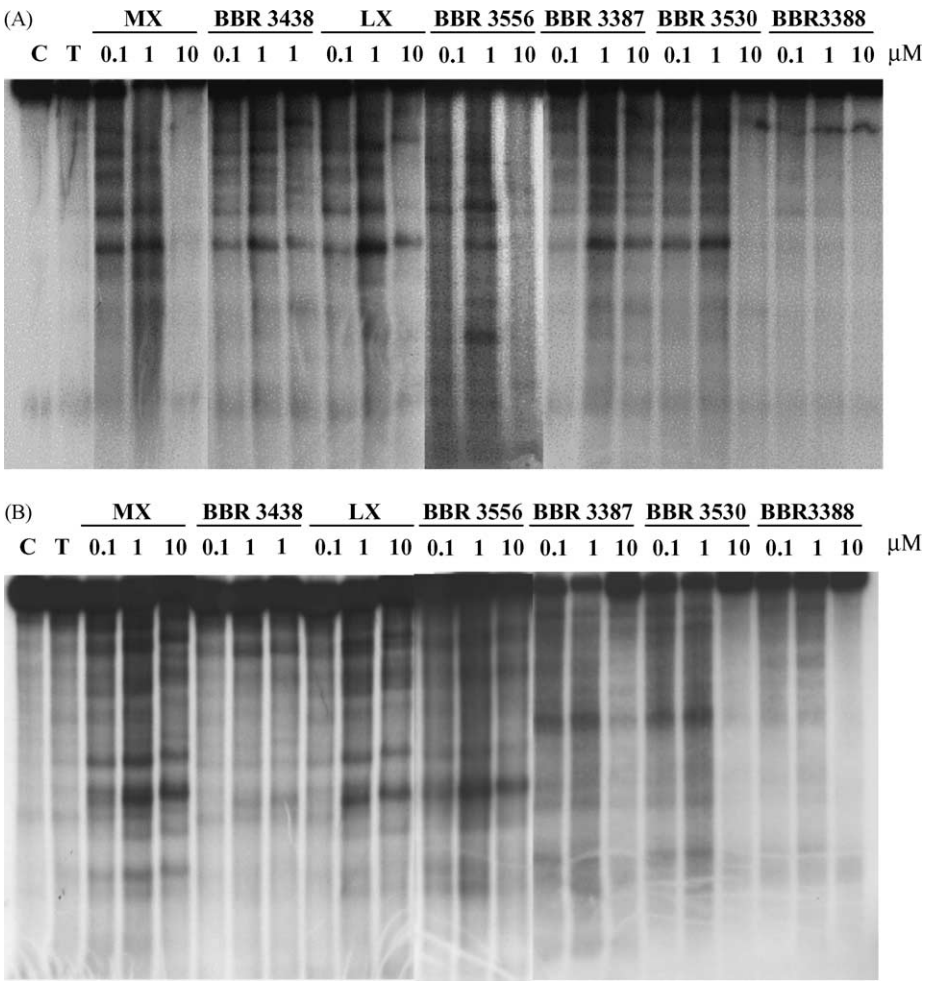

Fig. 7. Agarose gels of labeled pBR322 (50 ng) treated for 30 min with human DNA Topoisomerase II α (A) or β (B) in the absence or presence of test compounds at the indicated concentrations. Lane C refers to labeled DNA incubated without drugs or enzyme; lane T corresponds to enzyme digestion in the absence of drugs. LX: losoxantrone; MX: mitoxantrone.

These two hydroxylated anthrapirazoles showed a cutting site pattern completely superimposable to MX. No significant effects on top2α poisoning were found changing the side chains from primary to tertiary amine. Interestingly, derivatives carrying the nitrogen isosteric substitution at position 8 showed a profound reduction in poisoning ability as shown by the lack of detectable cleavage stimulation at all concentrations tested (Fig. 7A). To further evaluate the relevance of top2 poisoning to the aza-APs mechanism of action we investigated the drug-mediated stimulation DNA cleavage in the presence of top2β isoenzyme (Fig. 7B). The cleavage efficiency rank of drugs was essentially the same when comparing the α and β isoforms. Hence, no preference for poisoning one or the other human isoenzyme could be observed with the test aza-APs.

4. Discussion

The antineoplastic potency of aza-anthrapyrazoles is significantly related to the position of the C–N bioisosteric substitution. In fact, while the 9-aza derivatives are very effective drugs, two of them (BBR 3438 and BBR 3576) being at present in Phase II clinical trials, other regioisomers are devoid of anticancer activity [14,30]. In this work, several molecular properties of a large series of aza-APs have been investigated, and the results provide convincing evidence that: (i) the side chain of the drug can be a primary determinant of DNA binding affinity and specificity, and (ii) the clinical anticancer activity of the studied compounds is likely related to the potency in stimulating top2-mediated DNA breakage.

The physico-chemical properties of 8- and 9-aza congeners were examined in terms of electron distribution, protonation equilibria, molecular volume and shape, lipophilicity, self aggregation, and redox properties. The spectroscopic behavior of the two families in physiological solvent was very similar. In particular, neither group showed tendency to self-aggregation as it was the case for their carbocyclic counterparts. The molecular volume and surface area were practically the same in the 8- and 9-aza derivatives, ruling out steric parameters as possible discriminating factors. Acidity constants from potentiometric titrations as well as protonation and hydration energies were found to be quite comparable for the test regioisomers, indicating that the 8- and 9-aza species existing in solution display similar protonation and solvation equilibria. As far as hydrophobic properties are concerned, corresponding regioisomers gave practically identical estimates of log P values, ruling out differential hydrophobic effects as a possible cause of largely diverging pharmacological results.

Electron distribution data evaluated by quantum mechanical studies suggest that the local interchange between the atoms at positions 8 and 9 leaves the overall charge density practically unmodified. This was confirmed by the close values of the total dipoles in corresponding regioisomers. Moreover, the almost identical HOMO and LUMO energies did not suggest changes in the redox properties of the test aza-APs, ruling out differences in redox cycling as the possible source of the different biological responses.

The DNA-binding properties were also examined in great details. The 9-aza compounds showed a somewhat larger spread in the affinity for the nucleic acid as a function of the side chain substituents. In particular, the hydroxy-ethylamino-ethyl side arm characteristic of MX appeared to represent the best substituent at position 5, but not at position 2, where a shorter chain was preferred. These data are in line with the cell killing ability of 9-aza-APs since compounds BBR 3438 and BBR 3576 are the most potent drug candidates as shown by preclinical studies. Interestingly, oxidized derivatives either containing an N–O (BBR 3599) or a hydroxyl moiety in the aromatic system (BBR 3556) showed reduced DNA-binding propensity. The latter finding is at odd with the data reported for carbocyclic analogues, which showed enhanced binding when OH residues are introduced into the system [26,27]. The 8-aza congeners exhibited comparable affinities to DNA, the binding constants being close to the highest values found for the 9-aza counterparts. Hence, strength of DNA binding does not appear to account for the lack of activity in the 8-aza anthrapyrazoles. The orientation of the intercalated chromophore was then addressed by performing chiroptical measurements. Invariantly, aza-anthrapyrazole regioisomers gave a negative induced rotational strength at GC (and, when detectable, AT) steps. This suggests similar drug geometries in the complex of 8- and 9-aza-APs with DNA.

Sequence selectivity of the nucleic acid binding process was also examined. In general, the preference for GC steps is confirmed, as well as the remarkable lack of AT recognition by the derivatives having bulkier side arms. It is interesting to note that the nature of the side chains seems to be the key factor in improving GC sequence selectivity. In particular, only one hydroxyl ethyl side arm is compatible with remarkable GC step recognition. Again, when comparing 8- and 9-aza derivatives, no evident changes in base preference were observed. Hence, neither differences in affinity, nor in complex geometry, nor in base preference can be invoked to account for the pharmacological findings.

DNA top2 poisoning process was also considered using both α and β human isoforms. Interestingly, while the 9-aza-anthrapyrazoles succeeded in interfering with the enzyme, the 8-aza counterparts appeared to be essentially ineffective. Indeed, their poisoning ability was practically negligible especially in the presence of the α isoform. In agreement with our previous work, the bioisosteric C–N substitution at position 9 produced a lesser poisoning activity when compared to the carbocyclic system [15].

This occurred with both human isoforms, suggesting that top2 targeting is not isoform-specific using the aza compounds.

In conclusion, 8- and 9-aza-anthrapyrazoles show physico-chemical and DNA binding properties so similar that they cannot account for the biological differences discussed above. On the other hand, top2 poisoning effects are substantially separated in different regioisomers and correlate with their cancer cell killing ability. This points to an impaired interference with the DNA processing enzyme to explain the lack of cytotoxicity shown by the 8-aza compounds. Hence, cleavage complex recognition is dramatically affected when moving the nitrogen atom along the AP ring system. Considering that no major differences were monitored in the DNA-binding (and physico-chemical) properties, destabilizing (repulsive) contacts should occur between the 8-N and electronically similar residue(s) belonging to the protein. Considering that the observed poisoning effects follow the order carbocyclic $>$ 9-aza $>$ 8-aza, reduced electron density at position 9 and, even more, at position 8 would possibly improve drug interference with the cleavage complex and, hence, produce more potent APs derivatives. Another explanation of the substantial pharmacological difference between 8- and 9-APs possibly rests in a different drug recognition by metabolizing enzymes. Preliminary data indicate the presence of at least one major 9-aza-APs metabolite in PC3 cell extracts (unpublished results). Kinetic studies are warranted to clarify whether different rates of drug inactivation/activation could additionally contribute to the remarkable differences in anticancer potency exhibited by otherwise so similar aza-anthrapyrazoles.

Acknowledgments

This work has been carried out with financial support from Associazione Italiana per la Ricerca sul Cancro (AIRC), Milan, and the Italian Ministry for University and Research (MIUR), Rome, Italy.

References

[1] Krapcho AP, Maresch MJ, Hacker MP, Hazelhurst L, Menta E, Spinelli S, Beggiolin G, Giuliani FC, Pezzoni P, Tognella S. Anthracene-9,10-diones and aza bioisosteres as antitumor agents. Curr Med Chem 1995;2:803–24.

[2] Faulds D, Balfour JA, Chrisp P, Langtry HD. Mitoxantrone. A review of its pharmacodynamic and pharmacokinetic properties, and therapeutic potential in the chemotherapy of cancer. Drugs 1991;41: 400–49.

[3] Palumbo M, Gatto B, Sissi C. DNA topoisomerase-targeted drugs. In: Demeunynch M, Bailly C, Wilson WD, editors. DNA and RNA binders, vol. 1 from small molecules to drugs. Wiley-VCH; 2002. p. 503–37.

[4] Frishman WH, Sung HM, Yee HC, Liu LL, Keefe D, Einzig AI, Dutcher J. Cardiovascular toxicity with cancer chemotherapy. Curr Probl Cancer 1997;21:301–30.

[5] Krapcho AP, Landi Jr JJ, Hacker MP, McCormack JJ. Synthesis and antineoplastic evaluations of 5,8-bis[(aminoalkyl)amino]-1-azaanthracene-9,10-diones. J Med Chem 1985;28:1124–6.

[6] Krapcho AP, Petry ME, Getahun Z, Landi Jr JJ, Stallman J, Polsenberg JF, Gallagher CE, Maresch MJ, Hacker MP, Giuliani FC, Beggiolin G, Pezzoni G, Menta E, Manzotti C, Oliva A, Spinelli S, Tognella S. 6,9-Bis[(aminoalkyl)amino]benzo[g]isoquinoline-5,10-diones. A novel class of chromophore-modified antitumor anthracene-9,10-diones: synthesis and antitumor evaluations. J Med Chem 1994;37:828–37.

[7] Gandolfi CA, Beggiolin G, Menta E, Palumbo M, Sissi C, Spinelli S, Johnson F. Chromophore-modified antitumor anthracenediones: synthesis, DNA binding, and cytotoxic activity of 1,4-bis[(aminoalkyl)amino]benzo[g]-phthalazine-5,10-diones. J Med Chem 1995;38: 526–36.

[8] Faivre S, Raymond E, Boige V, Gatineau M, Buthaut X, Rixe O, Bernareggi A, Camboni G, Armand JP. A phase I and pharmacokinetic study of the novel aza-anthracenedione compound BBR 2778 in patients with advanced solid malignancies. Clin Cancer Res 2001; 7:43–50.

[9] Borchmann P, Schnell R, Knippertz R, Staak JO, Camboni GM, Bernareggi A, Hubel K, Staib P, Schulz A, Diehl V, Engert A. Phase I study of BBR 2778, a new aza-anthracenedione, in advanced or refractory non-Hodgkin's lymphoma. Ann Oncol 2001;12: 661–7.

[10] Dawson LK, Jodrell DI, Bowman A, Rye R, Byrne B, Bernareggi A, Camboni G, Smyth JF. A clinical phase I and pharmacokinetic study of BBR 2778, a novel anthracenedione analogue, administered intravenously, 3 weekly. Eur J Cancer 2000;36:2353–9.

[11] Showalter HDH, Johnson JL, Hoftiezer JM, Turner WR, Werbel LM, Leopold WR, Shillis JL, Jackson RC, Elslager EF. Anthrapyrazole anticancer agents. Synthesis and structure-activity relationship against murine leukemias. J Med Chem 1987;30:121–31.

[12] Talbot DC, Smith IE, Mansi JL, Hudson I, Calvert AH, Ashley SE. Anthrapyrazole CI-941: a highly active new agent in the treatment of advanced breast cancer. J Clin Oncol 1991;9:2141–7.

[13] Walsh SM, Walley WM, Chandra M, Huan SD, Veinot JP. Higginson LAJ, potential carditoxicity with the use of DuP-941: a case report. Can J Cardiol 1995;11:419–22.

[14] Krapcho AP, Menta E. Antitumor aza-anthrapyrazoles. Drugs Fut 1997;22:641–6.

[15] Sissi C, Moro S, Richter S, Gatto B, Menta E, Spinelli S, Krapcho AP, Zunino F, Palumbo M. DNA-interactive anticancer aza-anthrapyrazoles: biophysical and biochemical studies relevant to the mechanism of action. Mol Pharmacol 2001;59:96–103.

[16] Krapcho AP, Menta E, Oliva A, Di Domenico R, Fiocchi L, Maresch E, Gallagher CE, Hacker MP, Beggiolin G, Giuliani FC, Pezzoni G, Spinelli S. Synthesis and antitumor evaluation of 2,5-disubstituted-indazolo[4,3-gh]isoquinoline-6(2H)-ones (9-aza-anthrapyrazoles). J Med Chem 1998;41:5429–44.

[17] Beylin VG, Colbry NL, Goel OP, Haky JE, Johnson DR, Kanter GD, Leeds RL, Leja B, Lewis EP, Rithner CD, Showalter HDH, Sercel AD, Turner WR, Uhlendorf SE. Anticancer anthrapyrazoles. Improved synthesis of clinical agent CI-937, CI-941, and piroxantrone hydrochloride. J Heterocycl Chem 1989;26:85–96.

[18] Wells RD, Larson JE, Grant RC, Shortle BE, Cantor CR. Physicochemical studies on polydeoxyribonucleotides containing defined repeating nucleotide sequences. J Mol Biol 1970;54:465–97.

[19] Grant RC, Harwood SJ, Wells RD. The synthesis and characterization of poly d(I-C). J Am Chem Soc 1968;90:4474–6.

[20] Binaschi M, Farinosi R, Borgnetto ME, Capranico G. *In vivo* site specificity and human isoenzyme selectivity of two topoisomerase II-poisoning anthracyclines. Cancer Res 2000;60:3770–6.

[21] Cornarotti M, Tinelli S, Willmore E, Zunino F, Fisher LM, Austin CA, Capranico G. Drug sensitivity and sequence specificity of human recombinant DNA topoisomerases IIα (p170) and IIβ (p180). Mol Pharmacol 1996;50:1463–71.

[22] McGhee JD, Von Hippel PH. Theoretical aspects of DNA-protein interactions. Cooperative and non cooperative binding of large ligands to a one-dimensional homogeneous lattice. J Mol Biol 1974;86: 469–89.

[23] Chambers CC, Cramer CJ, Truhlar DG. A model for aqueous solvation based on class IV atomic charges and first-solvation-shell effects. J Phys Chem 1996;100:16385–98.

[24] Qui D, Shenkin S, Hollinger FP, Still WC. The GB/SA continuum model for solvation. A foot analytical method for the calculation of approximate born radii. J Phys Chem 1997;101: 3005–17.

[25] Hartley JA, Reszka K, Zuo ET, Wilson WD, Morgan AR, Lown JW. Characteristics of the interaction of anthrapyrazole anticancer agents with deoxyribonucleic acids: structural requirements for DNA binding, intercalation, and photosensitization. Mol Pharmacol 1988;33: 65–71.

[26] Denny WA, Wakelin LP. Kinetics of the binding of mitoxantrone, ametantrone and analogues to DNA: relationship with binding mode and anti-tumor activity. Anticancer Drug Des 1990;5:189–200.

[27] Lown JW, Morgan AR, Yen SF, Wang YT, Wilson WD. Characteristics of the binding of the anticancer agents mitoxantrone and ametantrone and related structures to deoxyribonucleic acids. Biochemistry 1985; 24:4028–35.

[28] Lyng R, Rodger A, Norden B. The CD of ligand-DNA systems. I. Poly(dG-dC) B-DNA. Biopolymers 1991;31:1709–20.

[29] Lyng R, Rodger A, Norden B. The CD of ligand-DNA systems. 2. Poly(dA-dT) B-DNA. Biopolymers 1992;32:1201–10.

[30] Supino R, Polizzi D, Pavesi R, Pratesi G, Guano F, Capranico G, Palumbo M, Sissi C, Richter S, Beggiolin G, Menta E, Pezzoni G, Spinelli S, Torriani D, Carenini N, Del Bo L, Facchinetti F, Tortoreto M, Zunino F. A novel 9-aza-anthrapyrazole effective against prostatic carcinoma xenografts. Oncology 2001;51:234–42.